Application of Response Surface Methodology for Optimization of Biodiesel Production from Microalgae Through Nanocatalytic Transesterification Process.

Vaishali Mittal
IIT Roorkee: Indian Institute of Technology Roorkee
Uttam Kumar Ghosh (uttam.ghosh@pe.iitr.ac.in)
IIT Roorkee: Indian Institute of Technology Roorkee https://orcid.org/0000-0001-5142-2586

Research Article

Keywords: biodiesel, microalgae, nanocatalyst, response surface methodology, fatty acid methyl esters, regression equation.

Posted Date: September 15th, 2021

DOI: https://doi.org/10.21203/rs.3.rs-771200/v1

Application of Response Surface Methodology for Optimization of Biodiesel Production from Microalgae Through Nanocatalytic Transesterification Process.

Vaishali Mittal and Uttam Kumar Ghosh*.

Department of Polymer and Process Engineering, IIT Roorkee, Roorkee-247667, Uttarakhand, India.

E-mail: uttam.ghosh@pe.iitr.ac.in

Abstract

Production of biodiesel from microalgae is gaining popularity since it does not compromise food security or the global economy. This article reports biodiesel production with *Spirulina* microalgae through nanocatalytic transesterification process. The nanocatalyst calcium methoxide $Ca(OCH_3)_2$ was synthesized using wet impregnation method and utilized to carry out the transesterification process. The nanocatalyst was characterized to evaluate its structural and spectral characteristics using different characterization techniques such as Thermogravimetric analysis (TGA), X-ray diffraction (XRD), Scanning electron microscopy (SEM), Fourier transform infrared spectroscopy (FT-IR), and Brunaeur-Emmett-Teller(BET) measurement for surface area. The result demonstrates that calcium methoxide $Ca(OCH_3)_2$ possesses a high catalytic activity compared to a heterogeneous catalyst such as calcium oxide (CaO). The impact of several process parameters such as reaction temperature, the molar ratio of methanol to oil, catalyst concentration, and reaction time used in the transesterification process was optimized by employing central composite design(CCD) based response surface methodology(RSM). The polynomial regression equation of second order was obtained for methyl esters. The model projected a 99% fatty acid methyl esters

(FAME) yield for optimal process parameters of reaction time 3hrs,3 wt.% of $Ca(OCH_3)_2$ catalyst loading, 80°C reaction temperature, and 30:1 methanol to oil molar ratio.

Keywords: biodiesel, microalgae, nanocatalyst, response surface methodology, fatty acid methyl esters, regression equation.

1. Introduction.

The concern about renewable energy is increasing in response to the rising carbon emissions and exhaustion of energy supplies through depleting fossil fuels (Tariq et al. 2012). Biodiesel is an impeccable alternative to petroleum-derived fuel, which could be generated from innumerable feedstocks such as edible or vegetable oils, woody plants, animal fat, or microalgae (Farobie and Matsumura 2017). Biodiesel is a biodegradable and sustainable clean fuel that minimizes nitrogen and sulfur pollutants in the exhaust gases and improves lubricity, flash point, and positive energy balance compared to conventional diesel (Knothe 2009). Biodiesel is a carbon-neutral biofuel produced by the chemical reaction called transesterification, where the triglycerides are converted to methyl esters of fatty acid in the existence of methanol and a catalyst, as shown in Eq. 1. (Atadashi et al. 2011). As biodiesel can be generated from various feedstocks but in densely populated nations like India, where food security is already a significant concern and demand for edible and non-edible oils is always high, microalgae is an ideal raw material for biodiesel production (Bojan et al. 2011).

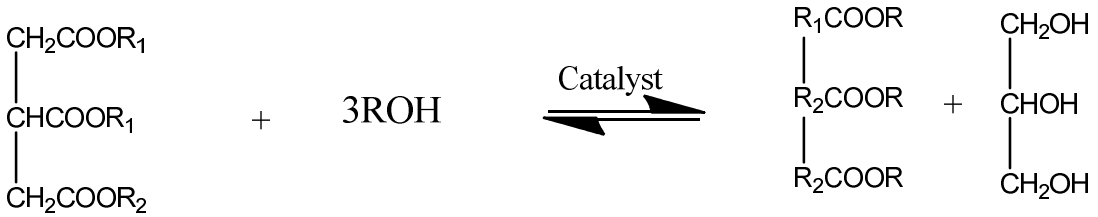

(1)

Microalgae is a unicellular organism distributed among fresh and seawater ecosystems with higher lipid content and yield than photosynthetic plants (Akubude et al. 2019). Algae-based biofuels have several advantages like the feedstock microalgae has fast-growing potential and are thus capable of producing biodiesel all year round, don't require any arable land, acts as a CO_2 sequestration device, and can produce non-toxic and eco-friendly fuel (Gendy and El-Temtamy 2013). Furthermore, microalgae can also be used to create some valuable co-products such as animal feed, proteins, lipids, pigments, vitamins, anti-oxidants, drugs, pharmaceuticals, etc. (Chen et al. 2018). In general, homogeneous and heterogeneous catalysts such as NaOH, KOH, lipases, and enzymes are utilized during the transesterification process. Still, currently, attention has been diverted towards the use of nanocatalyst because of its numerous advantages (Akubude et al. 2019).

Nanocatalysts may readily address the problems of mass transfer resistance, inefficiency, time consumption associated with the employment of homogeneous and heterogeneous catalysts because of their high specific surface area and catalytic activity. Nanocatalysts improve product quality and improve the yield efficiency at relatively moderate operating conditions (Akia et al. 2014). Moreover, nanocatalysts maintain their performance and thus can be reused up to 11 cycles. A number of studies have confirmed the improved biodiesel yield by the utilization of nanocatalysts. Fatty acid methyl esters of more than 95% were achieved by employing a nanomagnetic catalyst KF/CaO-Fe_3O_4 under ideal conditions, with catalyst reusability of up to 12-14 times without significant catalytic activity degradation(Hu et al. 2011). Transesterification of canola oil utilizing carbonated alumina doped with calcium oxide as a nanocatalyst yielded 98.8% biodiesel at optimum conditions of 270W microwave power, 15:1 methanol/oil ratio, 4 wt.% catalyst concentration, and 30minutes of reaction time (Nayebzadeh et al. 2018). FAME yield of

98.3% was achieved by utilizing solid acid nanocatalyst $TiO_2/PrSO_3H$ from transesterification of used cooking oil at 4.5 wt.% catalyst loading, 15:1 molar ratio, 60°C reaction temperature, and 9hr of reaction time (Gardy et al. 2017)

The response surface methodology is a statistical and mathematical procedure used to develop a functional relationship between various input variables and the response of interest (Khuri and Mukhopadhyay 2010). The significant advantage of utilizing RSM is that it produces the necessary statistics in fewer experimental runs (Bojan et al. 2011). RSM has previously been employed to study the optimization of biodiesel production from various feedstocks such as crude jatropha oil (Anr et al. 2016), soybean oil (Silva et al. 2011), and Jatropha curcas oil (Bojan et al. 2011).

In this article, biodiesel was produced by using *Spirulina* microalgae obtained from National Chemical Laboratory (NCL), Pune through the application of nanocatalyst $Ca(OCH_3)_2$ based transesterification and response surface methodology (RSM). The characteristics of nanocatalyst $Ca(OCH_3)_2$ were evaluated by using various instrumental techniques such as TG-DTA, FESEM, XRD, FT-IR, and BET surface area analysis. Further, central composite design (CCD) based response surface methodology was applied for better understanding the relationship between the several variables as reaction time, catalyst loading, the molar ratio of methanol to oil, the temperature of the reaction and response as defined in terms of the yield of methyl esters.

2. Materials and Methods.

2.1 Materials.

The microalgal strain of *Spirulina* was procured from the National Chemical Laboratory (NCL), Pune. Several chemicals such as calcium oxide (CaO), dried methanol (CH_3OH), chloroform ($CHCl_3$), and hexane(C_6H_{14}) were utilized for carrying out experimental work, and all the

chemicals or reagents used in the examination were of systematic grade. More than 90% purified calcium oxide was purchased from Merck Life sciences and specially dried methanol which was used as a biodiesel solvent. The hexane (C_6H_{14}) was purchased from Rankem chemicals, whereas chloroform($CHCl_3$) was acquired from Central Drug House (CDC) Ltd. Delhi. All the chemicals were utilized in their natural state, with no further purification.

2.2. Catalyst preparation.

The nanocatalyst calcium methoxide $Ca(OCH_3)_2$ was prepared by reacting 10gm of calcium oxide with 200ml of methanol (especially dried) at the desired temperature on a magnetic stirrer by continuously stirring at a rate of 600 rpm for 240 minutes. The continuous flow of nitrogen (N_2) gas or any other inert gas was provided to render the atmosphere inert. The reaction is shown in Eq. (2)

$$CaO + CH_3OH \rightarrow Ca(OCH_3)_2 + H_2O \quad (2)$$

The experiment was conducted in a three-neck round flask configuration fortified with a refluxing condenser and a magnetic stirrer. The efficient contact of reactants was ensured by continuous stirring at a rate of 600 rpm. The excess methanol was distilled using a rotary evaporator once the nanocatalyst was prepared.

2.3. Characterization of nanocatalyst.

The thermal stability of nanocatalyst was determined by using a thermogravimetric analyzer (TGA 55, TA Instruments, USA). The morphology and structure of nanocatalysts were investigated using field emission scanning electron microscopy (FESEM) on a MIRA3 TRESCAN operating at 5-6kV at room temperature. The X-ray diffraction (XRD) pattern of nanocatalyst was achieved using an ULTIMA IV RIGAKU, Japan diffractometer with a 40KV and 40 mA X-ray tube at ambient

temperature Cu Kα radiation (λ = 1.54 Å) to compute the crystalline size and crystalline planes. The samples were scanned at a rate of 2° /minute in the range of 2θ= 20-80°. To study functional groups present in the sample, Fourier Transform Infrared Spectroscopy (FTIR) spectra were collected (Make-Perkin Elmer, Model no.-L1600400 Spectrum) in the 4000-550 cm^{-1} range by utilizing pellets of potassium bromide (KBr). The total pore volume (cm^3/g), total surface area (S_{BET}), and average pore size (nm) of the catalyst were calculated by using the Brunauer-Emmett-Teller (BET) method. The specific surface area was calculated from the nitrogen adsorption/desorption branch of the isotherm using the equation of Brunauer-Emmett-Teller (BET) in a pressure range of 0.07-0.3 at 77K (Nova station A Quantachrome Instrument, USA). The desorption branches of the Barrett-Joyner-Halenda (BJH) plot were utilized to determine the distribution of pore size at a temperature of -196°C. Before the evaluation, the powdered sample was degassed at 200°C for 90 minutes under an inert or nitrogen atmosphere to eliminate moisture absorbed by the sample from the surrounding atmosphere.

2.4. Biodiesel production.

The production of biodiesel from microalgae through nanocatalytic transesterification by using $Ca(OCH_3)_2$ nanocatalyst comprises microalgal cultivation, harvesting, lipid extraction, and transesterification, as shown in Fig. (1)

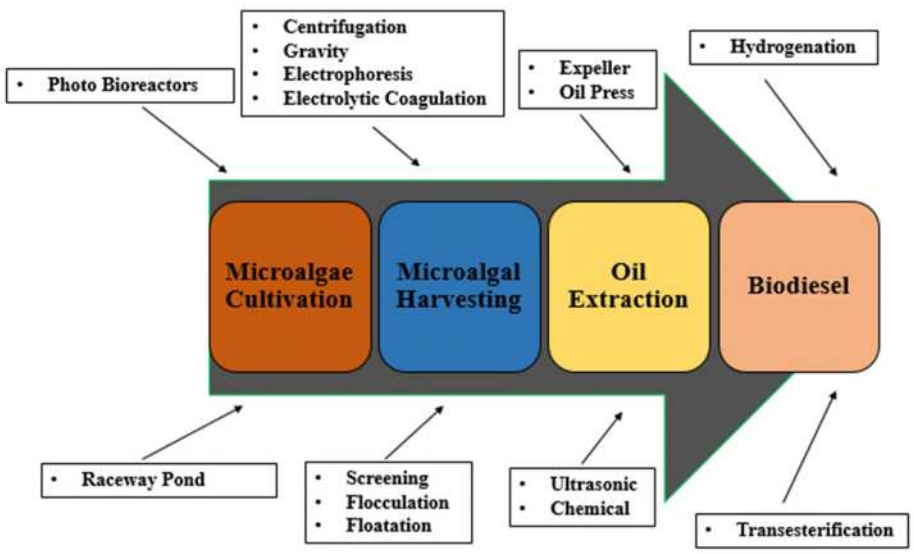

Fig. 1: Process flowchart for biodiesel production from microalgae.

2.3.1. Microalgae biomass preparation.

The microalgal strain of Spirulina was cultivated in a 1000 ml photobioreactor and maintained in ASN III media at 25 ± 2°C for a cultivation period of 14 days with 94.5 $\mu mol^{-2}s^{-1}$ light intensity of 16:08 dark and light cycle (Talapatra et al. 2021). Various techniques could harvest the microalgal biomass, but centrifugation was applied at a lab scale. The centrifugation process utilized centrifugal force to separate the concentrated microalgal biomass from the excess medium (Kiran et al. 2014). The widely used Bligh and Dyer method was employed to extract lipid by centrifuging the algal culture at 5000-7000 rpm for 10-12 minutes (Xu and Mi 2011). The supernatant was removed, and residual algal biomass was washed twice with deionized water and dried for 24 hrs. at 104°C in a vacuum oven. The resultant microalgal biomass was mixed with a (2:1v/v) chloroform: methanol solution in a 500ml conical flask and stirred continuously through the assistance of a magnetic stirrer. Once the reaction was accomplished, the products were clarified

149 or filtered and the required lipid was collected and kept in a glass bottle for the transesterification
150 reaction.

151 2.3.2. Transesterification reaction and FAME yield analysis.

152 The transesterification of the algal biomass was carried out in a three-necked round bottom flask
153 equipped with a water-cooled reflux condenser in the middle neck, and a thermometer in another
154 neck kept on a magnetic stirrer. The reaction was carried out at different methanol to oil molar
155 ratio (10:1, 20:1, 30:1, 40:1 and 50:1), catalyst loading (2, 2.5, 3, 3.5, and 4 wt.%), reaction
156 temperature (60, 70, 80, 90, and 100℃) and reaction time (120, 150, 180, 210, and 240 minutes).
157 A substantial quantity of oil, catalyst, and methanol were combined collectively and constantly
158 stirred on a hot plate at a constant temperature to initiate each reaction. After the reaction was
159 completed, three layers were achieved. The uppermost layer containing biodiesel had some solvent
160 thus collected and evaporated using a rotary evaporator.

161 The fatty acid methyl ester (FAME) yield was analyzed by using gas chromatography (GC)
162 equipped with mass spectroscopy (MS). A DB-5MS capillary column with a film thickness of
163 dimensions (30m×0.25m×0.25μm) was used in the experiment. In the experiment, helium was
164 employed as a carrier gas. The internal standard used for the analysis of biodiesel was methyl
165 heptadecanoate, and the solvent was hexane.

166 2.4. Factorial experimental design and optimization of parameters.

167 Central composite design (CCD) and Box-Behnken design (BBD) are the two most prevalent
168 experimental designs utilized in the response surface approach for optimization. In this study,
169 MINITAB software was used to apply the central composite design (CCD) design of RSM.
170 Furthermore, two essential models are generally used in RSM, i.e., the first-degree and second-

171 degree models (Khuri and Mukhopadhyay 2010). If the response can be well described through a
172 linear function of independent variables, the first-degree model is applied, but if the system has
173 curvature, a higher-degree polynomial, the second-order model, must be utilized. These models
174 establish the relationship between independent variables (time of reaction, methanol to oil ratio,
175 concentration of catalyst, and temperature of the reaction) and the dependent variable (methyl
176 esters). The experimental level and range of various independent variables for the production of
177 biodiesel are given in Table 1.

178 For this work, a set of 30 experimental runs were carried out, including 2^4 factorial/cube points, 8
179 axial/star points (α), and 6 center points. The illustration of factorial/cube points, axial/star, and
180 center points is shown in Fig 2. where "α" is the distance of star point from center points which is
181 equal to ($\alpha = 2^{n/4}$) where n is the factor number and for two factors α will be 1.414 ($\alpha = 2^{2/4} = 1.414$).

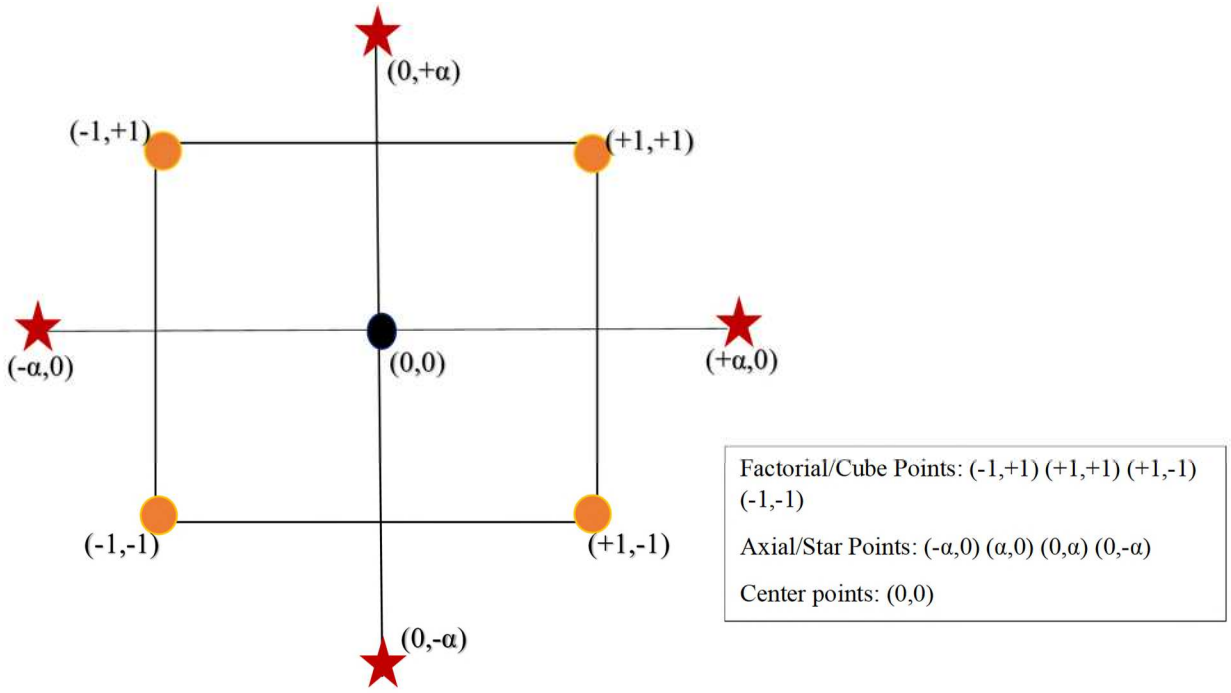

182

183 **Fig. 2:** Illustration of factorial, axial, and center points in CCD.

184 The second-degree model was employed in this article, which suggested 30 experimental runs
185 required for the procedure. As already discussed, this system observes a significant effect of
186 curvature. Hence, 8 more star experimental runs coded as α (runs 17-24) were added to the other
187 22 experimental runs, i.e., 2^4 factorial experimental runs (runs 1-16) and 6 center points (runs 25-
188 30) to craft central composite design.

189 **Table 1.** Independent variables experimental range and level.

Independent variable	Range and level				
	-α	-1	0	1	A
Molar ratio(x_1)	1.72:1	10:1	30:1	50:1	58.28:1
Concentration of catalyst (wt.%) (x_2)	1.586	2	3	4	4.414
Reaction Temperature (℃) (x_3)	51.72	60	80	100	108.28
Reaction time (min) (x_4)	95.16	120	180	240	264.84

190

191 For the design of an experiment for biodiesel production, the coded value of numerous independent
192 variables is given in Table 2. The x_1 and x_2 are the coded variable that denotes the molar ratio of
193 methanol to oil and the concentration or loading of catalyst, respectively. The coded variable x_3
194 and x_4 represents the temperature and the reaction time respectively.

195 The performance of this system is defined by the quadratic equation as stated in Eq. (3). The
196 statistical programme was used to perform a multiple regression data analysis. The optimum value
197 of selected variables can be attained by solving the regression equation and studying the response
198 surface and contour plot.

199 $$Y = \beta_0 + \sum_{j=1}^{k} \beta_j x_j + \sum_{i=1}^{k} \beta_{jj} x_j^2 + \sum \sum_{i<j}^{k} \beta_{ij} x_i x_j + \varepsilon \quad (3)$$

200 Where Y is the predicted response expressed as a percentage of methyl ester yield; x_i and x_j are the
201 actual independent variables in uncoded form; $\beta_0, \beta_j, \beta_{jj}$ and β_{ij} are intercept, linear, quadratic and
202 interaction constant coefficients respectively and ε is random error.

203 **Table 2**. Central composite design matrix for biodiesel production.

Run	**Independent variables**				**Point**	**Response**
	(x_1)	(x_2)	(x_3)	(x_4)		Methyl esters
1	-1	-1	-1	-1	Cube	6.9
2	+1	-1	-1	-1	Cube	32
3	-1	+1	-1	-1	Cube	65
4	+1	+1	-1	-1	Cube	85.4
5	-1	-1	+1	-1	Cube	47
6	+1	-1	+1	-1	Cube	53
7	-1	+1	+1	-1	Cube	50
8	+1	+1	+1	-1	Cube	75
9	-1	-1	-1	+1	Cube	42
10	+1	-1	-1	+1	Cube	70
11	-1	+1	-1	+1	Cube	50
12	+1	+1	-1	+1	Cube	77
13	-1	-1	+1	+1	Cube	49
14	+1	-1	+1	+1	Cube	81
15	-1	+1	+1	+1	Cube	61.6

16	+1	+1	+1	+1	Cube	82
17	-α	0	0	0	Axial	12.5
18	α	0	0	0	Axial	72
19	0	-α	0	0	Axial	60
20	0	A	0	0	Axial	92
21	0	0	-α	0	Axial	50
22	0	0	α	0	Axial	75
23	0	0	0	-α	Axial	65
24	0	0	0	A	Axial	72
25	0	0	0	0	Centre	70
26	0	0	0	0	Centre	99
27	0	0	0	0	Centre	88
28	0	0	0	0	Centre	87
29	0	0	0	0	Centre	92
30	0	0	0	0	Centre	97

3. Results and discussions.

3.1. Catalyst characterization.

3.1.1. Thermogravimetric analysis.

The thermal stability of nanocatalyst $Ca(OCH_3)_2$ was evaluated by using thermogravimetric analysis. The thermogravimetric analyzer was utilized to determine the weight loss of each sample at temperatures ranging from 35℃ to 800℃. The TG-DTA profile of the catalyst $Ca(OCH_3)_2$ is

shown in Fig. 3. In the temperature range of 35°C to 570°C, the TGA curve remains constant, with a slight loss of weight demonstrating the loss of moisture or volatile matter. The weight loss in the TGA curve occurs between the temperature range of 600°C to 800°C, which indicates the thermal decomposition of calcium carbonate however, the stable transition of CaO from $CaCO_3$ was caused at 668°C as confirmed from the DTA peak.

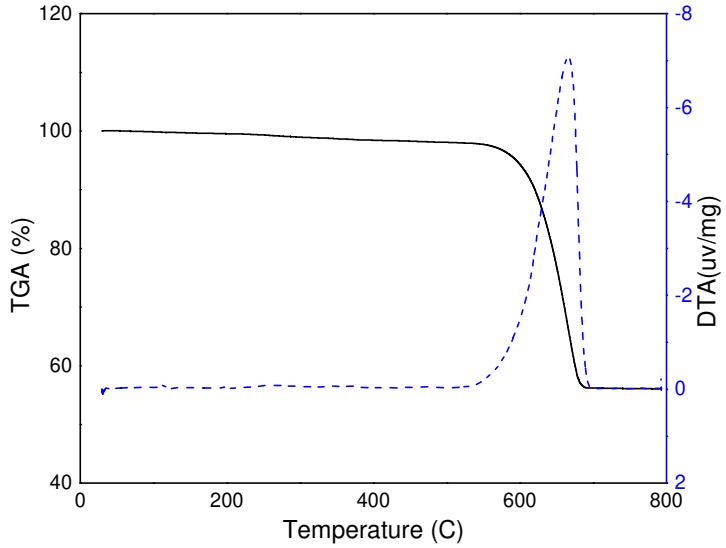

Fig. 3: TG/DTA profile of $Ca(OCH_3)_2$ nanocatalyst.

3.1.2. Scanning Electron Microscopy (SEM) comparison.

The sample is characterized by SEM to investigate the structure and morphology of nanocatalyst $Ca(OCH_3)_2$ images were taken at a working distance of 10-11 mm.

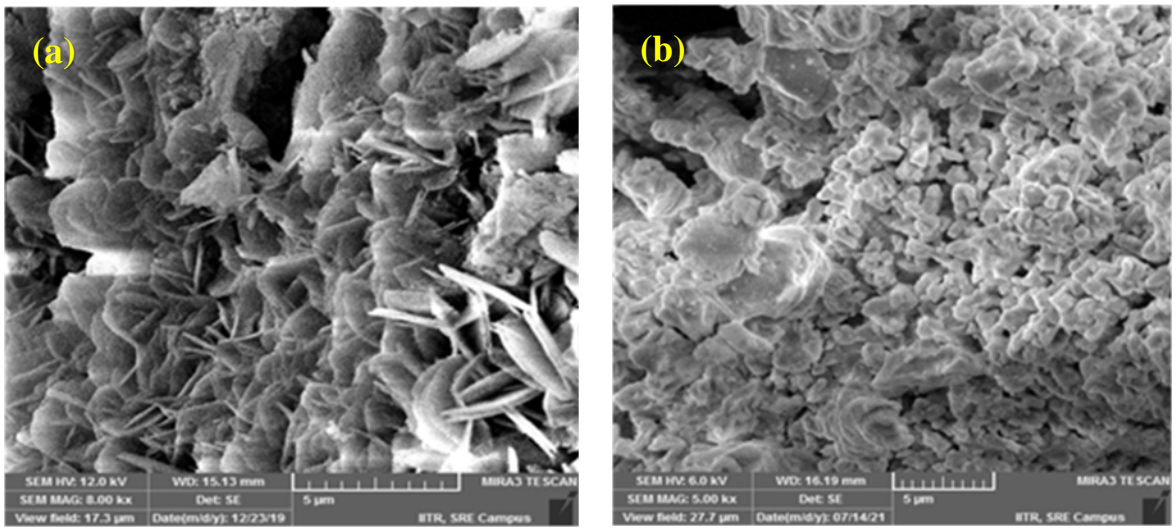

Fig. 4: FESEM (a) of $Ca(OCH_3)_2$ and (b) of CaO catalyst.

The SEM study supports the formation of nanoparticle $Ca(OCH_3)_2$ in flower shape with a particle size of 50nm, as shown in Fig. 4(a). In contrast, the asymmetrical profile of CaO could be due to the accumulation of bulk particles.

3.1.3. X-Ray Diffraction spectroscopy.

The XRD pattern is obtained to calculate the prepared sample's crystalline size and crystalline planes. The XRD pattern of CaO and calcium methoxide has been compared, as shown in Fig. (5).

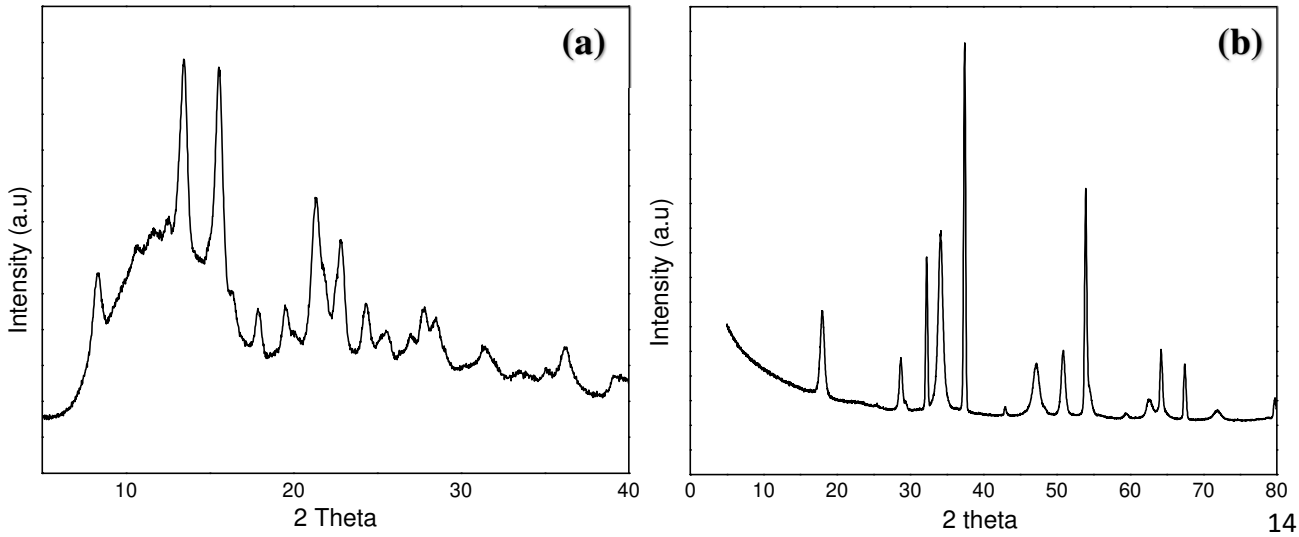

Fig. 5: XRD of (a) $Ca(OCH_3)_2$ and (b) CaO catalyst.

The firm peaks at 2θ ~37.34 and 32.23 corresponds to the calcium oxide d-values of 2.39 and 2.75 respectively, whereas peaks at 2θ ~34.18 and 18.16 belong to calcium hydroxide d-values of 2.62 and 4.88, respectively.

3.1.4. Fourier Transform Infrared Spectroscopy (FTIR)

FTIR spectrum was collected to investigate the functional group present in the sample. The essential functional groups of nanocatalyst $Ca(OCH_3)_2$ were visible in the FTIR spectrum at 1470 cm^{-1}, corresponding to the C-O stretch vibration of primary alcohol.

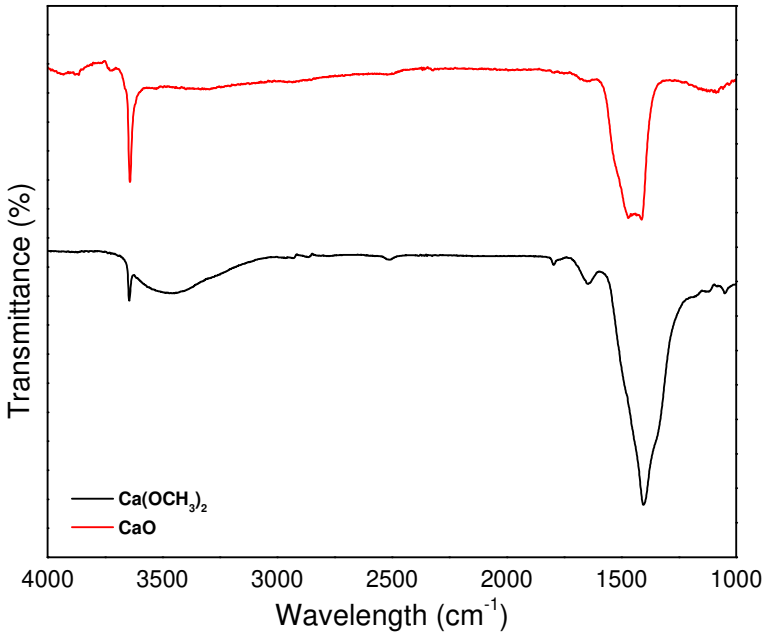

Fig. 6: FTIR of $Ca(OCH_3)_2$ and CaO catalyst.

The peak at 3650 cm^{-1} corresponds to stretching frequency due to CH_3 and may be due to moisture adsorption on the catalyst surface shown in Fig. 6. Furthermore; OH groups occurred as an isolated

material on the catalyst's surface, whereas in the FTIR spectrum of CaO catalyst no organic functional groups were found.

3.1.5. BET Surface area analysis.

The BET equation was employed to calculate the surface area from the adsorption/desorption branch of the isotherm in a pressure range of 0.07-0.3. Pore size distribution is determined from the BJH plot at -196°C temperature. The corresponding values for surface area, average pore size, and the pore volume of the nanocatalyst are 27.06 m^2/g, 1.188nm, and 0.024 $cm^3g^{-1,}$ respectively Fig. 7(b), and the surface area of $Ca(OCH_3)_2$ increases as shown in Table 3. which could increase the activity of transesterification reaction.

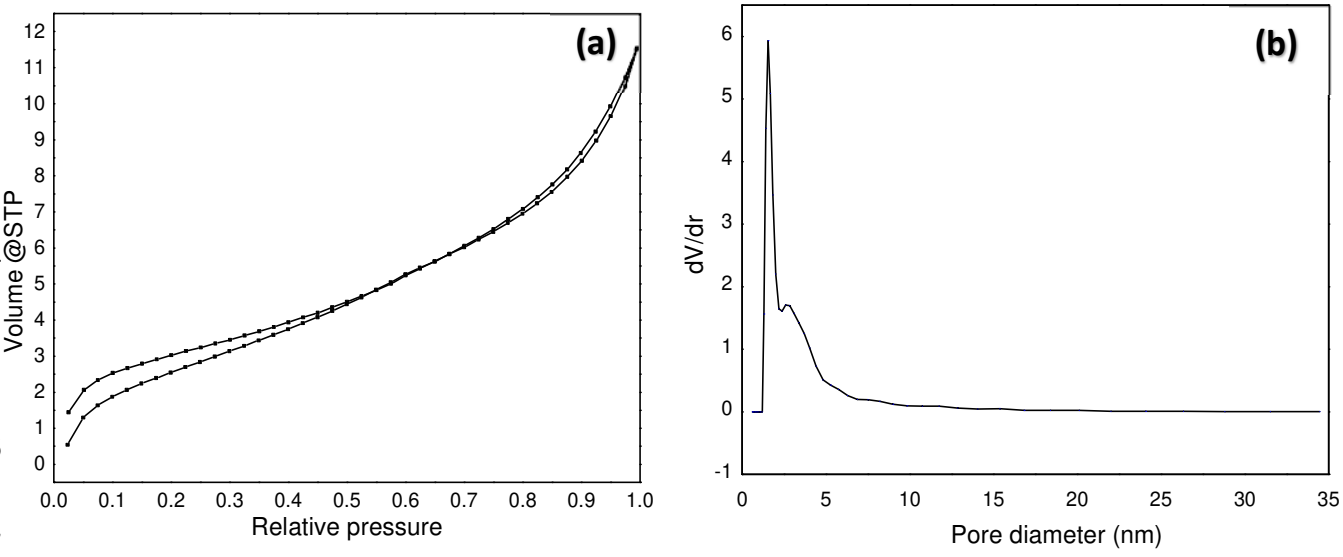

Fig. 7: (a) Nitrogen adsorption-desorption isotherm (b) pore size distribution of $Ca(OCH_3)_2$ catalysts.

Table 3. BET analysis of $Ca(OCH_3)_2$ and CaO catalysts.

Catalyst	CaO	$Ca(OCH_3)_2$
BET (m^2/g)	6.3	27.06
Pore volume (cm^3g^{-1})	0.0177	0.024
Pore diameter (nm)	3.12	1.188

281

282 3.2. Regression equation for methyl esters.

283 The four most critical parameters that impact the methyl esters yield are; the molar ratio of
284 methanol to oil (x_1), catalyst loading (x_2), reaction temperature (x_3), and reaction time (x_4). To
285 study the relationship between various parameters, the experimental runs were conducted by
286 varying physical variables. The empirical findings of the complete factorial central composite
287 design were fitted to the polynomial Eq. (3) using multiple regression analysis on Table 2. data.
288 The multiple regression equation for the methyl esters production as a function of the several
289 variables is shown in Eq. (4)

290 $$Y = -340.6 + 3.37x_1 + 58.4x_2 + 4.19x_3 + 0.856x_4 - 0.04322x_1^2 - 0.41x_2^2 - 0.01790x_3^2 -$$
291 $$0.0116x_4^2 - 0.017x_1x_2 - 0.00377x_1x_3 + 0.00124x_1x_4 - 0.297x_2x_3 - 0.1197x_2x_4 -$$
292 $$0.00042x_3x_4 \quad (4)$$

293 The effect of regression coefficients on the response is determined by the sign attached to the
294 coefficient. The negative sign indicates the combative impact, and the positive sign indicates the
295 coadjuvant result (Anr et al. 2016). Based on eq. (4) all four linear factors x_1, x_2, x_3, x_4 and the
296 interaction of x_1x_4 indicates the coadjuvancy effect whereas all the quadratic intercepts
297 $x_1^2, x_2^2, x_3^2, x_4^2$ and the interaction of $x_1x_2, x_1x_3, x_2x_3, x_2x_4$ and $x_3x_4$contributed to the combative
298 effect. Analysis of variance (ANOVA) was utilized to confirm the adequacy of the model, as given

299 in Table 4. At the 95% confidence level, the regression model exhibited a strong effect. The model
300 fit was tested using the coefficient of determination R^2, which was calculated to be 0.8588,
301 suggesting that the previously stated model could explain 85.88% of the response variability. In
302 this study, the transesterification experimental factors exhibited a total variation of 85.88% (R^2)
303 and an adj R^2 of 73.53%. This means that the model has a strong correlation and makes accurate
304 performance predictions. According to the ANOVA Table 4, the probability p-value is reported to
305 be 0.000. Still, it means that it is less than 0.001 and not exactly 0.000, indicating that the model
306 is significant precision and fitness.

307 **Table 4.** ANOVA (Analysis of Variance) for Methyl esters yield.

Source		**Degree of Freedom**	**Adj SS**	**Adj MS**	**F-value**	**P-value**
Regression		14	13485.9	963.28	6.95	0.000
	Linear	4	6473.5	1618.37	11.68	0.000
	Square	4	5546.6	1386.65	10.01	0.000
	Interaction	6	1465.9	244.31	1.76	0.171
Residual error		16	2217.2	138.57		
	Lack of fit	10	1677.2	167.72	1.86	0.230
	Pure error	6	540.0	90.00		
Total		30	15703.1			

308 "R^2=85.88% and adj R^2=73.53%

309 Further, it is noted from Pareto Chart, as shown in Fig. 8. that the molar ratio of methanol to oil
310 (x_1=4.95852), quadratic interaction of molar ratio ($x_2^2 = 4.50913$) and concentration of catalyst
311 ($x_2 = 3.86275$) had the highest impact on the yield of fatty acid methyl esters followed by the

interaction of catalyst loading and reaction time ($x_2x_4 = 2.44016$), the interaction of catalyst loading and reaction temperature ($x_2x_3 = 2.01542$) as well as reaction time (x_4 =1.992233), reaction temperature ($x_3 = 1.87393$), quadratic interaction of reaction temperature ($x_3^2 = 1.86738$) and quadratic interaction of reaction time ($x_4^2 = 1.08464$) whereas the interaction of molar ratio and temperature($x_1x_3 = 0.511818$), the interaction of molar ratio and reaction time ($x_1x_4 = 0.507571$), the interaction of reaction temperature and time ($x_3x_4 = 0.172022$), molar ratio, and catalyst loading ($x_1x_2 = 0.112558$), quadratic interaction of catalyst loading ($x_2^2 = 0.106210$) has a negligible impact as compared to other interactions.

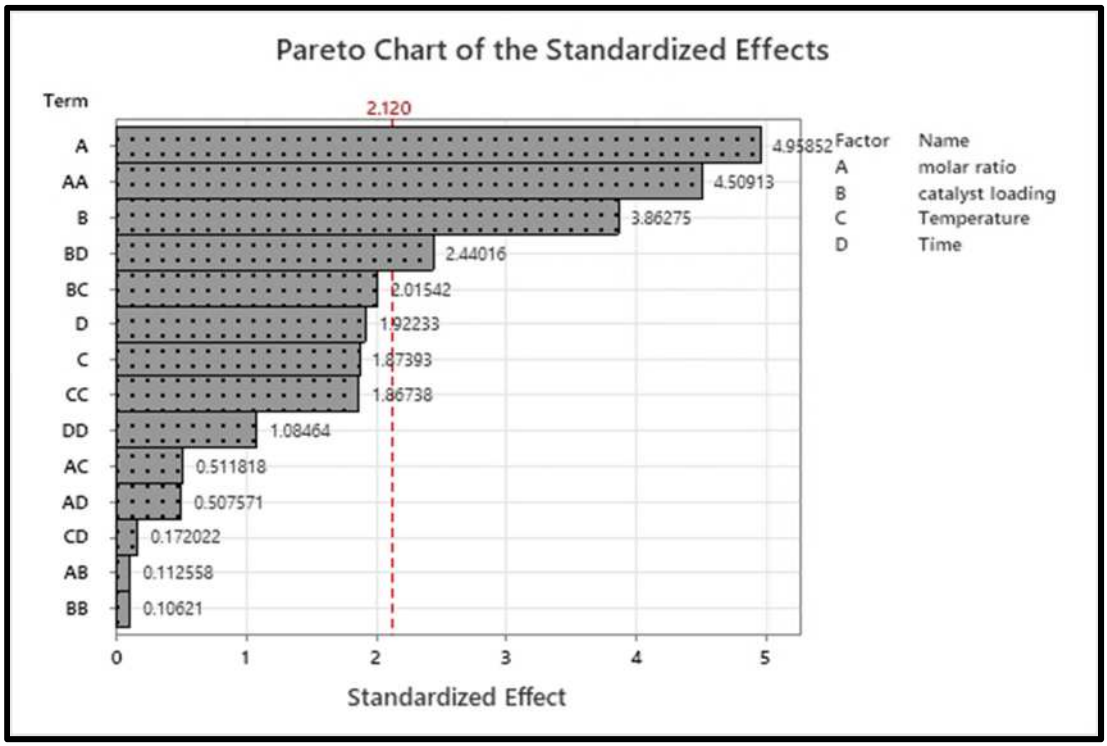

Fig. 8: Pareto chart of standardized effects on the production of methyl esters.

3.3. Impact analysis of transesterification parameters.

The distinguishing impact of transesterification parameters on the yield of methyl esters is depicted graphically in contour and surface plots. Figs. 9, 10, 11, and 12. Fig. 9 shows the clear impact of

the interaction of catalyst loading and molar ratio variables on the methyl esters yield. The 3D surface plot of Fig. 9 shows that the yield of methyl esters increases as the molar ratio of methanol to oil increases from 10:1 to 50:1, but the recovery of glycerol is difficult when there is too much alcohol present; therefore, the optimal methanol to oil ratio must be determined empirically after considering each process, and hence we found an optimum molar ratio of 30:1 for achieving a maximum yield of methyl esters (Silva et al. 2011; Zhang et al. 2020) Moreover, the biodiesel conversion was incomplete at the molar ratio of 10:1, and the higher molar ratio of 50:1 separation of glycerol becomes difficult (Teo et al. 2016) and hence the molar ratio of 30:1 considered to be appropriate. Similarly, we can also observe that the high methyl esters yield attained at a higher molar ratio and higher catalyst loading due to the availability of a higher number of active sites, but the excess use of a catalyst can cause emulsion (Hazmi et al. 2021) and hence the concentration of catalyst also theatres a significant role in improving the yield of biodiesel. Thus, maximum yield was obtained at the optimized condition with the molar ratio of 30:1 and catalyst loading of 3wt.%.

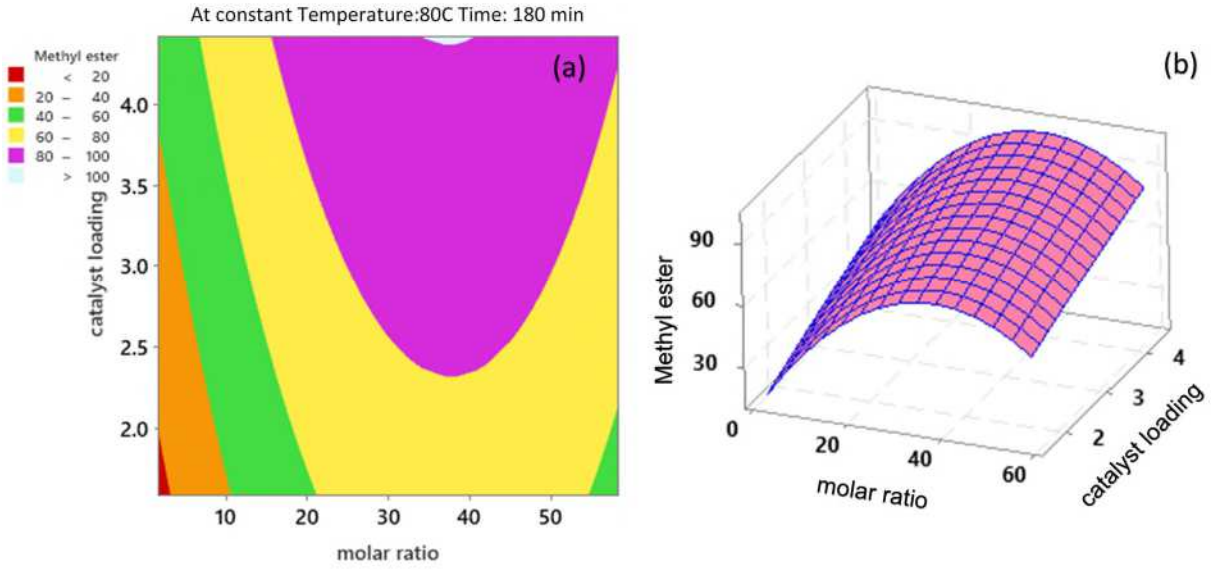

Fig. 9: (a) Contour plots and (b) surface plots of the interaction of catalyst loading and molar ratio.

Likewise, Fig. 10 displays the precise impact of the interactive factors of catalyst loading and temperature on the response yield of methyl esters. Fig. 11 depicts the response of interactive factors of molar ratio and temperature. The 3D response surface plots show that the yield of methyl ester increases as the temperature range increases from 60°C to 100°C because the rate of transesterification increases as the temperature increases due to the enrichment of miscibility of methanol and oil at higher temperatures (Teo et al. 2016). The optimum temperature was found out to be 80°C with optimum catalyst loading of 3wt.% for maximum yield of methyl esters.

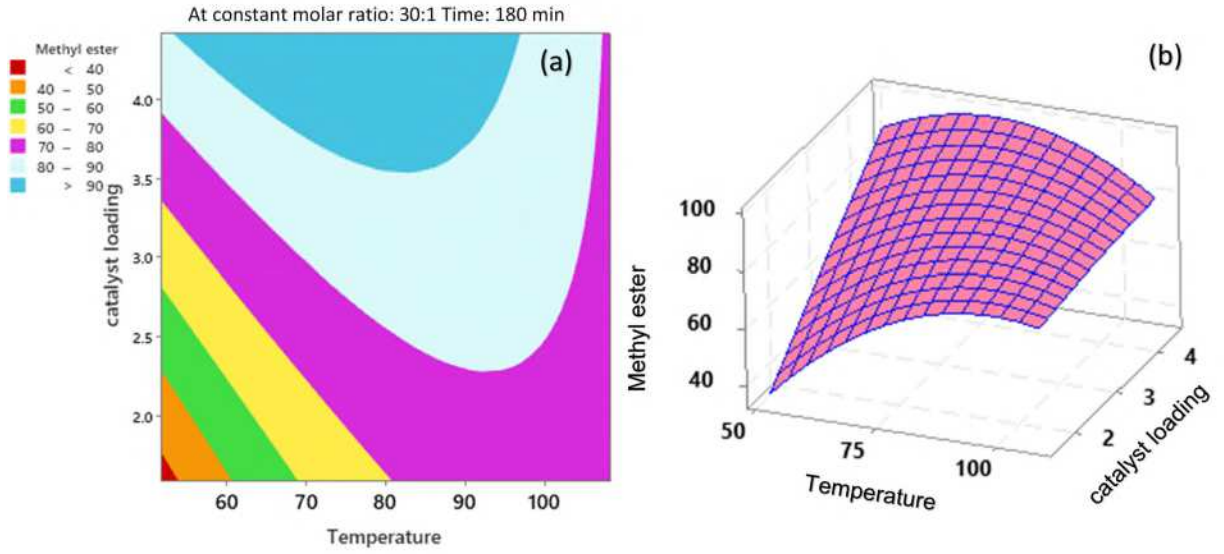

Fig. 10: (a) Contour plots and (b) surface plots of the interaction of catalyst loading and temperature.

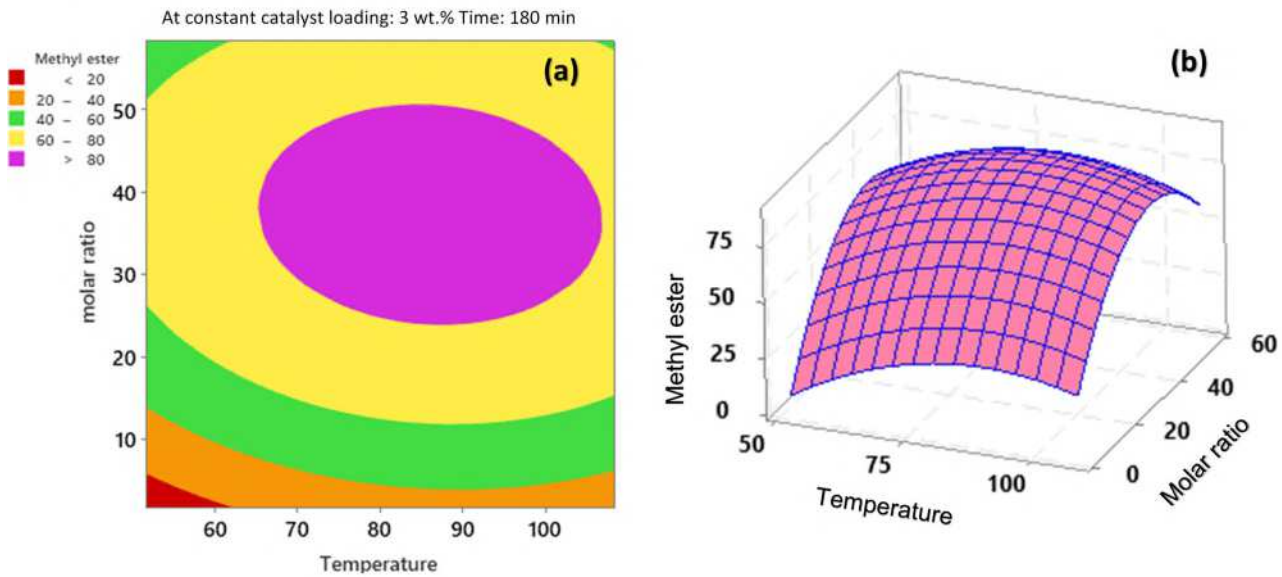

Fig. 11: (a) Contour plots and (b) surface plots of the interaction of molar ratio and temperature.

Fig. 12 depicts that the methyl esters yield is the function of molar ratio and time. The higher molar ratio results in faster conversion of biodiesel. However, the reaction time depends on the nature of the catalyst, and nanocatalyst usually requires a lesser time (1-2hrs) for conversion. The yield of methyl ester increases with the reaction time, but an excess reaction time can deteriorate the yield and lead to more glycerol production (Eevera et al. 2009). Hence, the optimum reaction time was 180 minutes, where the highest conversion was achieved.

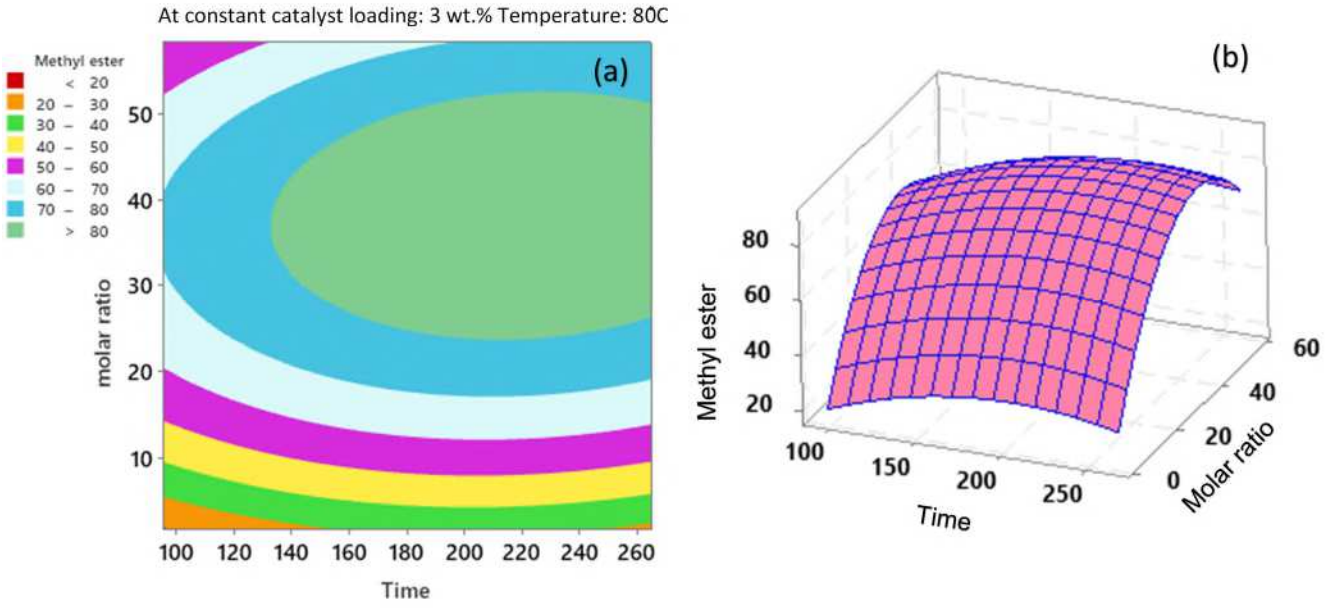

Fig. 12: (a) Contour plots and (b) surface plots of the interaction of molar ratio and time.

The optimum values of the selected variables can be calculated by solving the regression equation (4). The transesterification parameters such as the molar ratio of methanol to oil, catalyst loading, reaction temperature, and time were examined using contour plots, and the optimal values for attaining the maximum methyl esters yield were summarized. The transesterification parameters for the maximal methyl esters yield, which was determined to be 99%, were estimated using the Minitab simulated programme as molar ratio = 30:1 catalyst loading= 3wt.%, reaction

temperature= 80℃ and reaction time=180 minutes and were used for transesterification experimental validation. They yielded the best results, and hence after analyzing all the contour and 3D surface plots, we can conclude that the maximum yield of methyl esters obtained was 99% at a molar ratio of 30:1 at 3wt.% catalyst loading with reaction temperature of 80℃ and reaction time of 180 minutes.

The optimized values of the reaction parameters for maximal methyl esters production when a yield of 99% was attained are summarized in Table 5.

Table 5. Optimum parameter for maximum yield of methyl esters.

Parameters	**Optimum values**
Methyl esters (%)	99
Molar ratio (x_1)	30:1
Catalyst loading (wt.%) (x_2)	3
Temperature (℃) (x_3)	80
Time (minutes) (x_4)	180

4. Conclusions.

This research study concluded the formation of highly active nanocatalyst calcium methoxide $Ca(OCH_3)_2$ which was confirmed by the various structural and spectral characteristics. The TGA curve between the temperature range of 600°C to 800°C directs the thermal decomposition of calcium carbonate, whereas DTA peak at 668°C confirms the stable transition of calcium oxide (CaO) from calcium carbonate ($CaCO_3$). The SEM study shows the structure of nanocatalyst which is in the shape of flower with particle size of 50nm. The FT-IR spectrum endorses the presence of

386 essential functional groups in the nanocatalyst, which was evident at 1470 cm^{-1}. The BET surface
387 area analysis confirms the nanocatalyst with the high surface area of 27.06 m^2/g. The high specific
388 surface area of the nanocatalyst facilitates the interaction between catalyst and substrates, which
389 ultimately improves the efficiency of the nanocatalyst. The various variables which affected the
390 transesterification reaction were carried out at the laboratory scale.

391 The response surface methodology was used to study the effect of crucial parameters on converting
392 triglycerides to methyl esters. The process optimization was conducted by utilizing a central
393 composite design (CCD) based model of response surface methodology. The response surface
394 approach is an appropriate technique for optimizing operational parameters to increase the yield
395 of methyl esters. Transesterification reactions were carried out by utilizing CCD-based RSM,
396 where 30 experimental runs were successfully conducted for experimental design and analysis.
397 Graphical contour and surface plots were utilized to find the optimum point where the maximum
398 conversion of 99% was achieved at an optimum molar ratio of 30:1 methanol to oil, catalyst
399 loading of 3 wt.% at the reaction temperature of 80℃ and reaction time of 180 minutes. This result
400 demonstrates the novel synthesis process for a long-term solution with significant environmental
401 benefits for producing biodiesel.

402 **Declaration.**

403 **Ethics approval and consent to participate.**

404 Not applicable.

405 **Consent for publication.**

406 Not applicable.

Availability of data and materials.

Not applicable.

Competing interests.

The authors declare no competing interests.

Funding.

This research work is supported by the Department of Polymer and Process Engineering, IIT Roorkee, India. Financial support to execute this study is gratefully acknowledged to MHRD (Ministry of Human Resources Development) Plan Grant (2021-22) and IIT Roorkee (No. OH-35-71-142), IIT Roorkee, India.

Authors' contribution.

The manuscript was completed through contribution of all authors. Vaishali Mittal conceived the idea, performed the experimental and wrote the manuscript. Project administration, resources, validation, funding, acquisition was done by Uttam Kumar Ghosh.

All authors read and approved the final manuscript.

Acknowledgment.

The authors are grateful to support from the Department of Polymer and Process Engineering at Indian Institute of Technology Roorkee.

References.

Akia M, Yazdani F, Motaee E, et al (2014) A review on conversion of biomass to biofuel by

427 nanocatalysts. Biofuel Research Journal 1:16–25. https://doi.org/10.18331/BRJ2015.1.1.5

428 Akubude VC, Nwaigwe KN, Dintwa E (2019) Production of biodiesel from microalgae via
429 nanocatalyzed transesterification process: A review. Materials Science for Energy
430 Technologies 2:216–225. https://doi.org/10.1016/j.mset.2018.12.006

431 Anr R, Saleh AA, Islam MS, et al (2016) Biodiesel Production from Crude Jatropha Oil using a
432 Highly Active Heterogeneous Nanocatalyst by Optimizing Transesterification Reaction
433 Parameters. Energy and Fuels 30:334–343. https://doi.org/10.1021/acs.energyfuels.5b01899

434 Atadashi IM, Aroua MK, Aziz AA (2011) Biodiesel separation and purification: A review.
435 Renewable Energy 36:437–443. https://doi.org/10.1016/j.renene.2010.07.019

436 Bojan SG, Chelladurai S, Durairaj SK (2011) Response surface methodology for optimization of
437 biodiesel production from high FFA Jatropha curcas oil. International Journal of Green
438 Energy 8:607–617. https://doi.org/10.1080/15435075.2011.600373

439 Chen J, Li J, Dong W, et al (2018) The potential of microalgae in biodiesel production.
440 Renewable and Sustainable Energy Reviews 90:336–346.
441 https://doi.org/10.1016/j.rser.2018.03.073

442 Eevera T, Rajendran K, Saradha S (2009) Biodiesel production process optimization and
443 characterization to assess the suitability of the product for varied environmental conditions.
444 Renewable Energy 34:762–765. https://doi.org/https://doi.org/10.1016/j.renene.2008.04.006

445 Farobie O, Matsumura Y (2017) State of the art of biodiesel production under supercritical
446 conditions. Progress in Energy and Combustion Science 63:173–203.
447 https://doi.org/10.1016/j.pecs.2017.08.001

448 Gardy J, Hassanpour A, Lai X, et al (2017) Biodiesel production from used cooking oil using a
449 novel surface functionalised TiO2 nano-catalyst. Applied Catalysis B: Environmental
450 207:297–310. https://doi.org/10.1016/j.apcatb.2017.01.080

451 Gendy TS, El-Temtamy SA (2013) Commercialization potential aspects of microalgae for
452 biofuel production: An overview. Egyptian Journal of Petroleum 22:43–51.
453 https://doi.org/10.1016/j.ejpe.2012.07.001

454 Hazmi B, Rashid U, Ibrahim ML, et al (2021) Synthesis and characterization of bifunctional
455 magnetic nano-catalyst from rice husk for production of biodiesel. Environmental
456 Technology and Innovation 21:101296. https://doi.org/10.1016/j.eti.2020.101296

457 Hu S, Guan Y, Wang Y, Han H (2011) Nano-magnetic catalyst KF/CaO-Fe3O4 for biodiesel
458 production. Applied Energy 88:2685–2690. https://doi.org/10.1016/j.apenergy.2011.02.012

459 Khuri AI, Mukhopadhyay S (2010) Response surface methodology. Wiley Interdisciplinary
460 Reviews: Computational Statistics 2:128–149. https://doi.org/10.1002/wics.73

461 Kiran B, Kumar R, Deshmukh D (2014) Perspectives of microalgal biofuels as a renewable
462 source of energy. Energy Conversion and Management 88:1228–1244.
463 https://doi.org/10.1016/j.enconman.2014.06.022

464 Knothe G (2009) Improving biodiesel fuel properties by modifying fatty ester composition.
465 Energy and Environmental Science 2:759–766

466 Nayebzadeh H, Haghighi M, Saghatoleslami N, et al (2018) Fabrication of carbonated alumina
467 doped by calcium oxide via microwave combustion method used as nanocatalyst in
468 biodiesel production: Influence of carbon source type. Energy Conversion and Management

171:566–575. https://doi.org/10.1016/j.enconman.2018.05.081

Silva GF, Camargo FL, Ferreira ALO (2011) Application of response surface methodology for optimization of biodiesel production by transesterification of soybean oil with ethanol. Fuel Processing Technology 92:407–413. https://doi.org/10.1016/j.fuproc.2010.10.002

Talapatra N, Gautam R, Mittal V, Ghosh UK (2021) A comparative study of the growth of microalgae-bacteria symbiotic consortium with the axenic culture of microalgae in dairy wastewater through extraction and quantification of chlorophyll. Materials Today: Proceedings. https://doi.org/10.1016/j.matpr.2021.06.227

Tariq M, Ali S, Khalid N (2012) Activity of homogeneous and heterogeneous catalysts, spectroscopic and chromatographic characterization of biodiesel: A review. Renewable and Sustainable Energy Reviews 16:6303–6316. https://doi.org/10.1016/j.rser.2012.07.005

Teo SH, Islam A, Taufiq-Yap YH (2016) Algae derived biodiesel using nanocatalytic transesterification process. Chemical Engineering Research and Design 111:362–370. https://doi.org/10.1016/j.cherd.2016.04.012

Xu R, Mi Y (2011) Simplifying the process of microalgal biodiesel production through in situ transesterification technology. JAOCS, Journal of the American Oil Chemists' Society 88:91–99. https://doi.org/10.1007/s11746-010-1653-3

Zhang Y, Niu S, Lu C, et al (2020) Catalytic performance of NaAlO2/γ-Al2O3 as heterogeneous nanocatalyst for biodiesel production: Optimization using response surface methodology. Energy Conversion and Management 203:112263. https://doi.org/10.1016/j.enconman.2019.112263

490